Biocatalysis and Agricultural Biotechnology 17 (2019) 196–202

Contents lists available at ScienceDirect

Biocatalysis and Agricultural Biotechnology

journal homepage: www.elsevier.com/locate/bab

# Modeling of vitamin K (Menaquinoe-7) fermentation by *Bacillus subtilis natto* in biofilm reactors

Ehsan Mahdinia[a], Sina Jahangiri Mamouri[b], Virendra M. Puri[a], Ali Demirci[a,*], Aydin Berenjian[c]

[a] Department of Agricultural and Biological Engineering, The Pennsylvania State University, University Park, PA, 16802, United States
[b] Department of Mechanical Engineering, Michigan State University, East Lansing, MI 48824, United States
[c] Faculty of Science and Engineering, The University of Waikato, Hamilton 3240, New Zealand

ARTICLE INFO

*Keywords:*
MK-7
Menaquinone-7
Vitamin K
Biofilm reactor
*Bacillus subtilis*
Modeling

ABSTRACT

Menaquinoe-7 (MK-7) is the most potent form of vitamin K with numerous benefits for human health such as reducing the risks of cardiovascular diseases and osteoporosis in addition to having antitumor characteristics. Therefore, MK-7 production via bacterial fermentation has been studied intensely in the last few decades. Recently, biofilm reactors were implemented to enhance production levels in our lab. The specific objective of this study was to mathematically model the findings in batch biofilm reactors and thus further deepen our understanding of the conditions governing fermentation to pave the path to scaling up the production to pilot scale fermenters. The modified logistic equation was used to correlate substrate consumption with fermentation time and to model the substrate consumption in the four batch fermentations. Results indicated that this modified logistic model fits well with the experimental data for substrate consumption. Therefore there was no need for the other more complex models. Furthermore, this successfully modified-logistic equation was inserted into the Luedeking-Piret model to estimate MK-7 production based on substrate consumption, because of the typical MK-7 profiles in batch fermentations. There is sufficient evidence in the literature that MK-7 biosynthesis follows a mixed-metabolite pattern in *Bacillus subtilis natto*. Similarly, the modified-Gompertz model was used also for the same purpose. Results indicated that the modified Luedeking-Piret model fits more accurately for MK-7 production ($R^2$ = 0.971, 0.943, 0.970, and 0.959) compared to the modified-Gompertz ($R^2$ = 0.914, 0.943, 0.949 and 0.860).

## 1. Introduction

Shortly after the discovery of vitamin K (Dam, 1935), two major forms of vitamin K were identified (Widhalm et al., 2012). One is called phylloquinone, which is the plant form and found in most leafy green vegetables (Booth, 2012; Binkley et al., 1939). The other type is vitamin K2 type found in animal and microbial sources. Vitamin K2 includes 15 (most commonly 9) subtypes which are called menaquinones and are found in food sources such as red meat, egg yolk, and cheese as well as predominantly in microbial sources (Mahdinia et al., 2017a). Menaquinone-7 (MK-7) is the most potent microbial-produced form of vitamin K with extraordinary benefits for human health (Schurgers et al., 2007; Howard and Payne, 2006; Gast et al., 2009; Geleijnse et al., 2004; Yamaguchi, 2006). Extracting the vitamin from food sources is not practical; therefore, microbial fermentation on an industrial scale is the only feasible way to produce MK-7 (Berenjian et al., 2015).

*Bacillus subtilis natto* (Berenjian et al., 2011a, 2012, 2013, 2014), *Bacillus licheniformis* (Goodman et al., 1976) and *Bacillus amylolyquifaciens* (Wu and Ahn, 2011) are the most common strains studied for this purpose. Solid State Fermentation (SSF) and Liquid State Fermentation (LSF) strategies have been investigated for MK-7 production with *B. subtilis natto* (Singh et al., 2015; Wu and Ahn, 2011); yet, both SSF and static LSF strategies with no robust agitation and aeration, face serious scale-up, and operational issues (Pandey, 2003; Mahdinia et al., 2017a). Pellicle and biofilm formations that create these issues are on the other hand beneficial for the MK-7 biosynthesis (Ikeda and Doi, 1990). Switching to LSF strategies with agitation and aeration creates the platform for more efficient scale-up strategies, but decimates the pellicle and biofilm formations. With the opportunity to use biofilm reactors to harness the biofilm formations and keep these benefits and at the same time have robust agitation and aeration, biofilm reactors were constructed with suitable Plastic Composite Support (PCS) and strain combination and growth conditions and medium compositions were optimized using the Response Surface Methodology (RSM) (Mahdinia

* Corresponding author.
*E-mail address:* demirci@psu.edu (A. Demirci).

https://doi.org/10.1016/j.bcab.2018.11.022
Received 24 April 2018; Received in revised form 8 October 2018; Accepted 21 November 2018
Available online 22 November 2018
1878-8181/ 

et al., 2018a, 2018b, 2018c, 2018d).

However, there is a need to mathematically model the MK-7 production and substrate consumption in these batch biofilm reactors to further elucidate the larger scale fermentation strategies (Mahdinia et al., 2018e). Logistic function model is originally utilized to model biomass growth. Then, Luedeking–Piret and Gompertz equations were used to correlate product formation to biomass growth and substrate consumption and also to model substrate consumption in relation to biomass production. Coban and Demirci (2016) used modified versions of Gompertz and logistic models to predict lactic acid production and glucose consumption in lactic acid fermentation by *Rhizopus oryzae*. Also, logistic model was applied to calculate batch kinetics of microbial growth for polysaccharide production (Mohammad et al., 1995). Moreover, Mohammad et al. (1995) described pullulan production with the modified-Luedeking–Piret model and modified-Gompertz model. Similarly, Cheng et al. (2010) modified logistic, Gompertz, and Luedeking–Piret models to explain pullulan fermentation by using a color variant strain of *Aureobasidium pullulans* in biofilm reactors. Results indicated that the modified Gompertz models proposed in the study demonstrated its flexibility to fit all biomass production, pullulan production, and sucrose consumption. Mahanama et al. (2012) also assumed the Luedeking–Piret model in correlation with biomass growth on solid state substrate to explain MK-7 biosynthesis by *B. subtilis natto* in tray fermenters. In this study, however, direct correlation of MK-7 production with substrate consumption is targeted for batch biofilm reactors as a further step towards scaling-up MK-7 fermentation in agitated liquid state fermenters.

## 2. Materials and methods

### 2.1. Microorganisms and media

*Bacillus subtilis natto* (NF1) was isolated from commercial natto, as previously described (Mahdinia et al., 2017b). For biofilm formation in the biofilm reactor, Plastic Composite Supports (PCS) were used as described by Mahdinia et al. (2017b). The fermentation media consisted of 10 g of soytone (Difco, Detroit, MI), 5 g of yeast extract (Difco), 45 g of glycerol (EMD Chemicals, Gibbstown, NJ) and 0.6 g of $K_2HPO_4$ (VWR, West Chester, PA) for the glycerol-based medium and 3 g of soytone (Marcor, Carlstadt, NJ), 5 g of NaCl (EMD), 2.5 g of $K_2HPO_4$ (VWR) and 152.6 g of glucose (Tate & Lyle), 17.6 g of casein (tryptone) (Marcor) and 8 g of yeast extract (Biospringer), per liter of deionized water, as concluded by our previous studies (Mahdinia et al., 2018c).

### 2.2. Biofilm reactors

Sartorius Biostat B Plus twin system bioreactors (Allentown, PA) equipped with 2-L vessels (1.5-L working volume) were utilized. Sterile 4 N sulfuric acid (EMD) and 4 N sodium hydroxide (Amresco, Solon, OH) along with antifoam B emulsion (Sigma-Aldrich, Atlanta, GA) were added automatically to maintain pH and suppress foaming as needed. The PCS tubes type SFYB (50% Polypropylene, 35% soybean hulls, 5% soybean flour, 5% yeast extract, 5% bovine albumin and salts) were manufactured and implemented (Ho et al., 1997) and biofilm reactors for glycerol and glucose-based media were operated at optimum conditions as described in previous studies (Mahdinia et al., 2018a, 2018b).

For biofilm formations to form on the PCS grids, bioreactors were set up with grid-like fashion PCS formations. Then, sterile medium was added to the bioreactors and refreshed for four times (Mahdinia et al., 2018a). Growth parameters (temperature (30–45 °C)), pH (6 − 8) and agitation(100–234 rpm) and medium compositions were used as determined in our previous studies (Mahdinia et al., 2018a, 2018b, 2018c, 2018d).

### 2.3. Analysis

#### 2.3.1. MK-7 analysis

Fermentation broth sample (3 ml) was mixed with 2:1, v/v n-hexane:2-propanol mixture to extract the MK-7 content (Berenjian et al., 2011b). N-hexane:2-propanol (2:1, v/v) with 1:4 (liquid:organic, v/v) was used for MK-7 extraction from the broth. The mixture was vigorously shaken using a vortex mixer for 3 min and then the organic phase was separated and evaporated under forced air flow at ambient temperature. Then, dried pellets containing the MK-7 were dissolved in methanol in a Biosonic ultra-sonication water bath (Cuyahoga Falls, OH) for 15 min at ambient temperature. After the pellets were completely suspended in methanol, the mixtures were filtered through 0.2 μm PTFE filters (PALL Life Sciences, Port Washington, NY). MK-7 concentrations in the samples were then analyzed by High Performance Liquid Chromatography (HPLC) using UV–Vis light as described in previous studies (Mahdinia et al., 2017b; Shahami et al., 2017).

#### 2.3.2. Substrate analysis

Samples of the fermentation broth were centrifuged at 9000 × *g* for 5 min (Microfuge 20 Series, Beckman Coulter Inc., Brea, CA) and then filtered through 0.2 μm cellulosic filters (PALL). Then, with no dilution, the cell-free broth was analyzed by HPLC as described the previous studies (Mahdinia et al., 2018a).

#### 2.3.3. Statistical and mathematical analysis

Growth and medium main effects along with the 2nd order and two-way interaction effects were obtained using Minitab 17.0 ANOVA (Minitab Inc., State College, PA) with statistical model and regression analysis with Box-Cox transformation optimal λ (λ equal to 1 or 0.5). A confidence level of 95% was implemented throughout the analysis procedures to distinguish significant parameters (Rahimi et al., 2017a, 2017b).

### 2.4. Mathematical models

MATLAB software package (R2017a, MathWorks, Natick, MA) was used to carry out mathematical calculations and fits. Modified Logistic equation was applied for modeling the substrate consumptions. Modified Gompertz and modified Luedeking–Piret equations were derived and used to model MK-7 productions. Models for MK-7 productions and the model for substrate consumptions were developed using the average results of optimum growth conditions and medium compositions obtained in previous studies (Mahdinia et al., 2018a, 2018b, 2018c, 2018d). Table 1 depicts the nomenclatures used in this study.

#### 2.4.1. Modeling for substrate consumption

Bacterial cells utilize the substrate available to them to grow, reproduce, and maintain, and besides these, biosynthesize numerous metabolites. The substrate consumption curves, in which substrate concentrations are plotted versus time of fermentation, usually exhibit sigmoid patterns including a lag phase followed by an exponential phase and finally a stationary phase. Although sigmoid functions such as the logistic equation (Eq. (1)) have been originally developed and modified for modeling growth curves (Zwietering et al., 1990); yet further-modified versions of the Logistic equation have been developed for substrate consumptions (Kargi, 2009):

$$-\frac{dS}{dt} = kS\left(1-\frac{S}{S_0}\right) \quad (1)$$

In Eq. (1), $k$ is the specific substrate consumption rate. Integrating Eq. (1) while considering $S_{(t=0)} = S_0$ and if $\tau \gg 0$ then defining $S_{(t=\tau)} = \frac{S_0}{2}$ and finally $S_{(t=\infty)} = 0$,the following equation is obtained:

$$S_{(t)} = \frac{S_0}{1+e^{k(t-\tau)}} \quad (2)$$

**Table 1**
Nomenclatures used in this study.

| Symbol | Name | Value | Unit | Equations |
|---|---|---|---|---|
| $k_s$ | Specific substrate consumption rate | | $h^{-1}$ | (1),(2),(4) |
| $k_p$ | Specific MK-7 production rate | | $h^{-1}$ | |
| $k_{p\text{-}m}$ | Max specific MK-7 production rate | | $h^{-1}$ | (5) |
| $k_{s\text{-}A}$ | Specific substrate consumption rate for glycerol growth | 0.030 | $h^{-1}$ | |
| $k_{p\text{-}mA}$ | Max specific MK-7 production rate for glycerol growth | 0.133 | $h^{-1}$ | |
| $k_{s\text{-}B}$ | Specific substrate consumption rate for glucose growth | 0.062 | $h^{-1}$ | |
| $k_{p\text{-}mB}$ | Max specific MK-7 production rate for glucose growth | 0.179 | $h^{-1}$ | |
| $k_{s\text{-}C}$ | Specific substrate consumption rate for glycerol medium | 0.054 | $h^{-1}$ | |
| $k_{p\text{-}mC}$ | Max specific MK-7 production rate for glycerol medium | 0.175 | $h^{-1}$ | |
| $k_{s\text{-}D}$ | Specific substrate consumption rate for glucose medium | 0.059 | $h^{-1}$ | |
| $k_{p\text{-}mD}$ | Max specific MK-7 production rate for glucose medium | 0.120 | $h^{-1}$ | |
| S | Substrate concentration (glycerol or glucose) | | g/L | (1–4) |
| $S_0$ | Initial substrate concentration | | g/L | (1),(2), (4) |
| $S_{0\text{-}A}$ | Initial glycerol concentration for glycerol growth | 43.2 | g/L | |
| $S_{0\text{-}B}$ | Initial glucose concentration for glucose growth | 140.3 | g/L | |
| $S_{0\text{-}C}$ | Initial glycerol concentration for glycerol medium | 45.6 | g/L | |
| $S_{0\text{-}D}$ | Initial glucose concentration for glucose medium | 128.4 | g/L | |
| P | Product concentration | | mg/L | (3),(5) |
| $P_0$ | Initial product concentrations | 0 | mg/L | |
| $P_m$ | Max product concentration | | mg/L | (5) |
| $P_{m\text{-}A}$ | Max product concentration for glycerol growth | 12.1 | mg/L | |
| $P_{m\text{-}B}$ | Max product concentration for glucose growth | 18.5 | mg/L | |
| $P_{m\text{-}C}$ | Max product concentration for glycerol medium | 14.7 | mg/L | |
| $P_{m\text{-}D}$ | Max product concentration for glucose medium | 20.5 | mg/L | |
| t | Time | | h | (1–5) |
| $\tau$ | Time of max specific substrate consumption rate | | h | (2),(4) |
| $\tau_A$ | Time of max specific substrate cons. rate for glycerol growth | 72 | h | |
| $\tau_B$ | Time of max specific substrate cons. rate for glucose growth | 48 | h | |
| $\tau_C$ | Time of max specific substrate cons. rate for glycerol medium | 48 | h | |
| $\tau_D$ | Time of max specific substrate cons. rate for glucose medium | 48 | h | |
| e | Constant | 2.710 | | (2),(4),(5) |
| $\lambda$ | Lag time for MK-7 production | | h | (5) |
| $\lambda_A$ | Lag time of MK-7 production for glycerol growth | 24 | h | |
| $\lambda_B$ | Lag time of MK-7 production for glucose growth | 12 | h | |
| $\lambda_C$ | Lag time of MK-7 production for glycerol medium | 12 | h | |
| $\lambda_D$ | Lag time of MK-7 production for glucose medium | 0 | h | |
| $\alpha$ | First Modified-Leudeking–Piret constant | | mg/g | (3),(4) |
| $\beta$ | Second Modified-Leudeking–Piret constant | | mg/g/h | (3),(4) |
| $\alpha_A$ | First Modified-Leudeking–Piret constant for glycerol growth | − 0.250 | mg/g | |
| $\beta_A$ | Second Modified-Leudeking–Piret constant for glycerol growth | 0.00065 | mg/g/h | |
| $\alpha_B$ | First Modified-Leudeking–Piret constant for glucose growth | − 0.088 | mg/g | |
| $\beta_B$ | Second Modified-Leudeking–Piret constant for glucose growth | 0.00041 | mg/g/h | |
| $\alpha_C$ | First Modified-Leudeking–Piret constant for glycerol medium | − 0.089 | mg/g | |
| $\beta_C$ | Second Modified-Leudeking–Piret constant for glycerol medium | 0.00301 | mg/g/h | |
| $\alpha_D$ | First Modified-Leudeking–Piret constant for glucose medium | − 0.138 | mg/g | |
| $\beta_D$ | Second Modified-Leudeking–Piret constant for glucose medium | 0.00010 | mg/g/h | |

In Eq. (2), $S_0$ is the initial substrate concentration, $\tau$ is the time of fermentation when specific substrate consumption rate ($k_s$) is maximum and $t$ is the time elapsed in fermentation. This integrated form (Eq. (2)) is the Logistic equation for substrate consumption independent of biomass concentrations. Such an equation is capable of presenting a sigmoidal curve of substrate (in this case glycerol or glucose) concentrations throughout fermentation period with empirical representation of the lag, log and stationary phases.

### 2.4.2. Modeling for production

The product (MK-7) biosynthesis in this study is described by two models. First is the Luedeking–Piret model. In this regard, product biosynthesis rate is considered dependent upon both instantaneous substrate concentration $S$ and substrate consumption rate $dS/dt$ in a linear fashion:

$$\frac{dP}{dt} = \alpha\frac{dS}{dt} + \beta S \tag{3}$$

where $\alpha$ and $\beta$ are empirical constants that vary dependent on fermentation conditions and are determined to best-fit the experimental values.

Thus, a good estimation of the product biosynthesis would be to insert Eq. (1) and Eq. (2) into Eq. (3) and integration using MATLAB with the assumption of $P_{(t=0)} = P_0 = 0$ we have:

$$P_{(t)} = \frac{\alpha S_0}{1+e^{k(t-\tau)}} - \beta S_0\left[t - \frac{ln(e^{k(t-\tau)}+1)}{k}\right] - \frac{\alpha S_0}{e^{-k\tau}+1} + \frac{\beta S_0 ln(e^{-k\tau}+1)}{k} \tag{4}$$

The Luedeking–Piret equation was originally developed to explain fermentation kinetics of glucose to lactic acid secretion based on instantaneous rate of bacterial growth and to the bacterial density (Luedeking and Piret, 1959). However, modifying it so that production rate correlates directly to instantaneous substrate consumption rate and substrate concentration was attempted here; since the Luedeking-Piret equation is effective in modeling mixed-metabolite products such as organic acids or in this case MK-7 (Leh and Charles, 1989).

On the other hand, a modified-Gompertz function that was previously successful in modeling bacterial cellulose was also evaluated in this study as well (Cheng et al., 2010):

$$P_{(t)} = P_m exp\left\{-exp\left[\frac{k_{m-p}e}{p_m}(\lambda - t)+1\right]\right\} \tag{5}$$

where $P_m$ is the maximum product (MK-7) concentration in each batch,

$k_{m-p}$ is the maximum specific production rate in each batch and $\lambda$ is the lag time for production.

## 3. Results and discussions

Models for glycerol or glucose consumptions and MK-7 production were constructed using the repeated data obtained from four batch fermentation runs under optimum growth parameters in glycerol-based medium, growth parameters in glucose-based medium, medium components in glycerol-based medium and medium components in glucose-based medium (Mahdinia et al., 2018a, 2018b, 2018c, 2018d). These four batch fermentation results included different ranges of pH, temperature, agitation and media components in glycerol and glucose-based media. All models were developed in a way to reflect relevant biological parameters such as specific growth rate, specific production rate, lag time, etc. Using these terms, the models were implemented to fit the experimental values of substrate and product concentrations during the fermentations. In order to evaluate the models, R-squared ($R^2$) values, Root-Mean-Square Errors (RMSE) and Mean Absolute Errors (MAE) between modeled values and experimental values were obtained. Moreover, experimental vales were plotted versus the corresponding values from the models and the slope of the best fitted trendline was obtained. The constant values $k_p$, $k_s$, T, $\lambda$, $\alpha$ and $\beta$ were empirically assumed to best fittings.

### 3.1. Substrate consumption models

Modified-logistic model as described in Eq. (2) was used to obtain predicted fits for glycerol and glucose concentrations in the four batches. These values along with the experimental values were plotted versus time (Fig. 1). The modified-logistic model fitted to the experimental values well ($R^2 > 0.953$) and since this model is a very simple and parsimonious one, unlike previous studies, there was no need to look into more complex models such as the Gompertz model (Cheng et al., 2010c). Also, it is shown in Fig. 1 that the glycerol consumption in the glycerol growth plot is unlike the other three graphs. In this case, glycerol was not depleted at all (Fig. 1A), whereas substrate completely depleted in the other cases by the fourth or fifth day of the fermentations (Fig. 1B, C, and D). It is obvious from Fig. 1 that the consumption pattern is unique for glycerol growth optimization run, possibly, because the medium is much richer in nutrients compared to others (Mahdinia et al., 2018a). Thus, $\tau = 72h$ was more proper for the glycerol growth case while $\tau = 48h$ was used for the other cases simply because maximum specific substrate consumption rates occurred sooner in those cases perhaps because in the rich and complex glycerol

**Table 2**
Model validations for substrate consumptions.

| Model | RMSE (g/L) | MAE (g/L) | $R^2$ | Slope |
|---|---|---|---|---|
| Modified-Logistic for glycerol growth | 2.7 | 2.4 | 0.953 | 1.08 |
| Modified-Logistic for glucose growth | 5.1 | 4.1 | 0.991 | 1.02 |
| Modified-Logistic for glycerol medium | 2.4 | 1.8 | 0.981 | 1.07 |
| Modified-Logistic for glucose medium | 5.1 | 3.5 | 0.989 | 1.03 |

- RMSE was calculated as the square root of the sum of differences between predicted substrate concentrations and observed values.
- MAE was calculated as sum of absolute differences between predicted substrate concentrations and observed values.
- $R^2$ was calculated as proportion of the variance in the observed substrate concentrations predictable from the modeled values.
- Slope was calculated as the slope of the trending line drawn over observed substrate concentrations plotted versus predicted values.

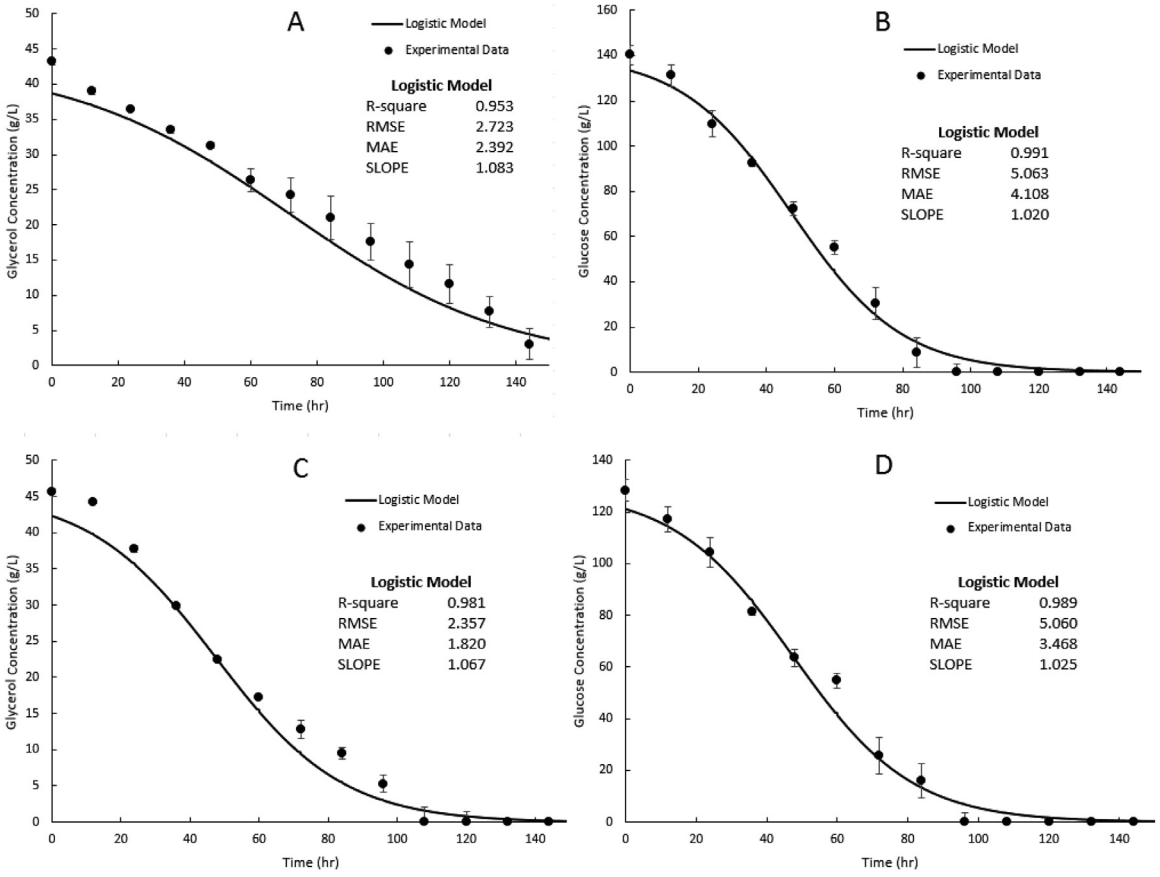


**Fig. 1.** Experimental values and fitted Modified-Logistic models for substrate concentrations in batch fermentations for glycerol growth optimization (A), glucose growth optimization (B), glycerol medium optimization (C) and glucose medium optimization (D).

medium, metabolism was significantly slower in general. Concordantly, the specific substrate consumption rates applied for Fig. 1A is considerably lower ($k = 0.030$) than the values for Fig. 1B, C, and D, which were very close (0.062, 0.054 and 0.059, respectively). Table 2 indicates that for glucose consumptions, RMSE (5.1 and 5.1 g/L) and the MAE values (4.1 and 3.5 g/L) are significantly higher than the amounts for glycerol consumptions (2.7, 2.4 and 2.4, 1.8 g/L, respectively); yet, the $R^2$ values for glycerol consumptions (0.953 and 0.981) are also lower than those of the glucose consumption models (0.991 and 0.989). In other words, although RMSE and MAE values for glycerol consumption model are lower than glucose model, glucose consumptions are modeled more accurately by the models. This is simply because the amount of glucose consumed are over or nearly 3 times the amount of glycerol and therefore the RMSE and MAE values are not directly comparable. Nonetheless, all models for substrate consumptions are very accurate ($R^2 > 0.953$) and were sufficient to be applied for MK-7 production models.

### 3.2. MK-7 production models

Experimental MK-7 concentrations and the model values from the modified-Luedeking–Piret and modified-Gompertz models for all four batches were plotted as shown in Fig. 2. As it is depicted in Fig. 2A, B, and C for glycerol and glucose growth and glycerol medium fermentations, the modified-Gompertz models showed better fit to the experimental values compared to the glucose medium fermentation (Fig. 2D). The reason is more obvious in Table 3 where $R^2 = 0.836$ was obtained for Fig. 2D, whereas for others, the $R^2$ values were significantly higher (0.914, 0.943 and 0.950). The RMSE, MAE, and slope comparisons also indicate a significant difference. The RMSE for Fig. 2D is equal to 2.5 g/L for the modified-Gompertz model, but those values for Fig., 2A, B, and C are equal to 1.0, 1.4 and 1.0 g/L respectively. Same as MAE values where 2.0 g/L is compared to 0.9, 1.3, and 0.8 g/L and slope, where 1.44 is compared with 0.87, 0.97, and 0.88. The RMSE and MAE values are true comparisons because there are no differences in the scale of the MK-7 concentration in the fermentations. Such a lack of accuracy for Fig. 2D is perhaps coming from the low maximum specific production rate and is also evident when the lag time is observed which is equal to zero in this case. It means that the MK-7 is being biosynthesized form the very beginning of the fermentation, which is simply not true and some lag time always exist, even in biofilm reactors (Ercan and Demirci, 2013).

On the other hand, the modified-Luedeking–Piret equation was fair to all four models. Once again, lower RMSE (0.6, 1.5, 0.8, and 1.5 mg/L) and MAE values (0.4, 1.2, 0.7, and 1.3 mg/L) meant higher $R^2$ values (0.971, 0.943, 0.970, and 0.959), which therefore suggest more accurate models. In general, modified-Luedeking–Piret equation was more accurate than the modified-Gompertz equation in modeling MK-7 production as evident from $R^2$ values (0.971 vs 0.914, 0.943 vs 0.943, 0.970 vs 0.943 and 0.959 vs 0.863 for modified-Luedeking–Piret vs modified-Gompertz, respectively). This is naturally because the modified-Luedeking–Piret equation and the Luedeking–Piret equation in general are more competent and even specific to modeling mixed-metabolites such as the MK-7 in this case (Luedeking and Piret, 1959). Also, the modified-Luedeking–Piret equation possesses three fitting parameters (α, β, and τ) whereas the modified-Gompertz equation only has one (λ). Thus, although modified-Gompertz model is a more parsimonious model, it is not accurate and, therefore, effective for modeling MK-7 biosynthesis. The reason for the modified-Gompertz model to have a very low precision in the case of the glucose medium optimization batch data ($R^2 = 0.863$) is due to a low $k_m$ value. The maximum specific production rate in this case was substantially lower than the other counterpart batches. Visually, it is also obvious that the slope at the turning point of the product profile is smoother and therefore the specific rate was lower. If the production rate was as high as expected by the model, its precision would be higher because the model is tuned with all four batch cases and not just glucose medium optimization results. Also, it can be noted that the modified-logistic model was not as accurate in modeling product profiles as compared to substrate consumption. This is due to the fact that the logistic model was originally

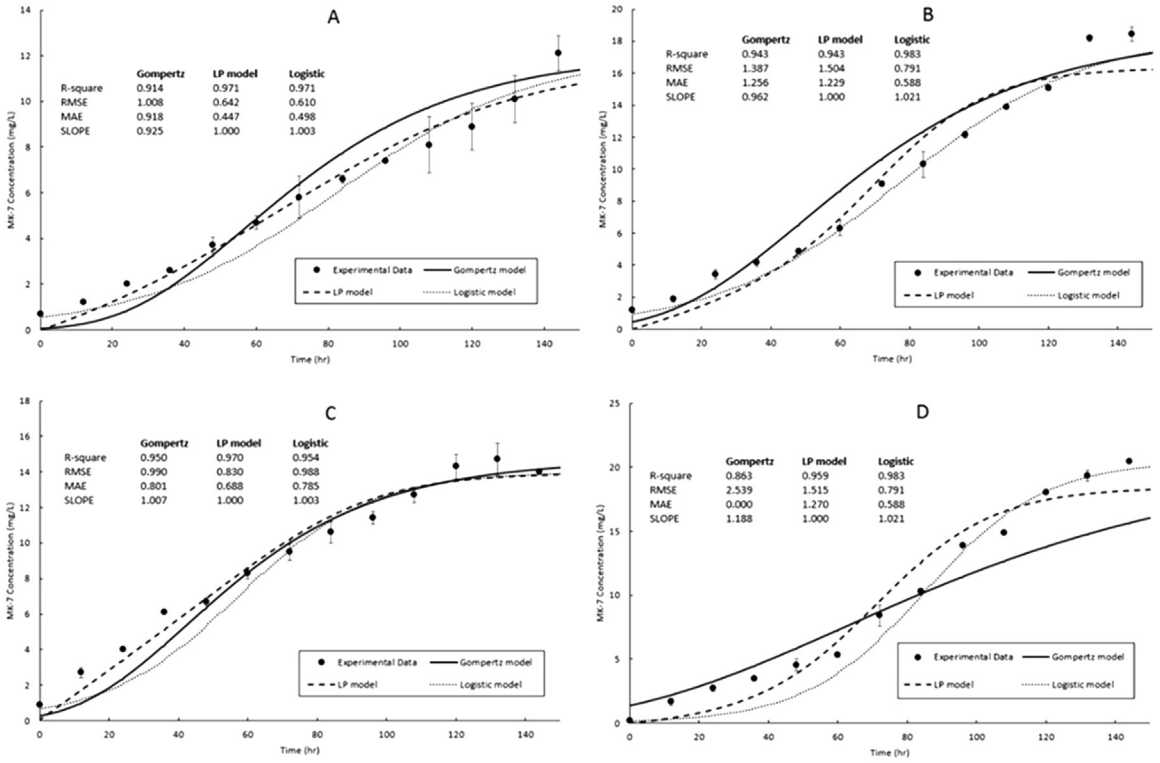


**Fig. 2.** Experimental values and fitted Modified logistic, Modified-Gompertz and Modified-Leudeking–Piret models for MK-7 production in batch fermentations for glycerol growth optimization (A), glucose growth optimization (B), glycerol medium optimization (C) and glucose medium optimization (D).

**Table 3**
Validation for MK-7 productions.

| Model | RMSE (mg/L) | MAE (mg/L) | $R^2$ | Slope |
|---|---|---|---|---|
| Modified-Leudeking–Piret for glycerol growth | 0.6 | 0.5 | 0.971 | 1.00 |
| Modified-Gompertz for glycerol growth | 1.0 | 0.9 | 0.914 | 0.93 |
| Modified-logistic for glycerol growth | 0.6 | 0.5 | 0.971 | 1.00 |
| Modified-Leudeking–Piret for glucose growth | 1.5 | 1.2 | 0.943 | 1.00 |
| Modified-Gompertz for glucose growth | 1.4 | 1.3 | 0.943 | 0.96 |
| Modified-logistic for glucose growth | 0.8 | 0.6 | 0.983 | 1.02 |
| Modified-Leudeking–Piret for glycerol medium | 0.8 | 0.7 | 0.970 | 1.00 |
| Modified-Gompertz for glycerol medium | 1.0 | 0.8 | 0.949 | 1.01 |
| Modified-logistic for glycerol medium | 1.0 | 0.8 | 0.954 | 1.00 |
| Modified Leudeking–Piret for glucose medium | 1.5 | 1.3 | 0.959 | 1.00 |
| Modified-Gompertz for glucose medium | 2.5 | 2.0 | 0.863 | 1.19 |
| Modified-logistic for glucose medium | 0.8 | 0.6 | 0.983 | 1.02 |

- RMSE was calculated as the square root of the sum of differences between predicted MK-7 concentrations and observed values.
- MAE was calculated as sum of absolute differences between predicted MK-7 concentrations and observed values.
- $R^2$ was calculated as proportion of the variance in the observed MK-7 concentrations predictable from the modeled values.
- Slope was calculated as the slope of the trending line drawn over MK-7 substrate concentrations plotted versus predicted values.

developed for population growth or resource consumption modeling purposes. Thus, while it can be used for products such as MK-7, since the product is a function of substrate consumption, the indirect effects naturally reduces the effectiveness of the modified-logistic model.

## 4. Conclusions

In this study, substrate (glycerol and glucose) consumptions and product biosynthesis (MK-7) in four batch fermentations were modeled. RMSE, MAE, $R^2$ and slopes for predicted values versus experimental values were obtained to evaluate models. For substrate consumptions, a modified-Logistic equation was implemented and the accuracy of the models were high enough to overrule any needs for more complex models ($R^2$ values of 0.953, 0.981, 0.991, and 0.989). The modified-Logistic models were inserted in the modified-Luedeking–Piret equation and integrated, then with a modified-Gompertz equation, MK-7 productions were modeled. Results indicated that naturally, the modified-Luedeking–Piret equation ($R^2$ values of 0.9705, 0.943, 0.970, and 0.959) was more accurate in modeling the MK-7 production compared to the modified-Gompertz model ($R^2$ values of 0.914, 0.943, 0.9425, and 0.863). Thus, considering typical MK-7 profiles in batch fermentations, there is no doubt that MK-7 biosynthesis follows a mixed-metabolite pattern in *Bacillus subtilis natto*. The next step in boosting MK-7 fermentation in liquid state would be scaling up the process to pilot scale fermenters. This can be challenging as many factors and conditions change in the transition from the 2-L biofilm reactors used in our recent studies to 100-L or larger pilot-scale fermenters. In this regard, these accurate mathematical models obtained in this study and perhaps applying secondary models such as neural network or root square models to these findings in future studies, would be valuable in providing prevision of the scale up process.

## Acknowledgments

This work was supported by the USDA National Institute of Food and Agriculture Federal Appropriations under Project PEN04561 and Accession number 1002249. The authors thank the Statistical Consulting Center at The Pennsylvania State University for their support in providing useful consultation for data processing.

## References

Berenjian, A., Mahanama, R., Kavanagh, J., Dehghani, F., 2015. Vitamin K series: current status and future prospects. Crit. Rev. Biotechnol. 35, 199–208. https://doi.org/10.3109/07388551.2013.832142.

Berenjian, A., Mahanama, R., Talbot, A., Biffin, R., Regtop, H., Kavanagh, J., 2011a. The effect of amino-acids and glycerol addition on MK-7 production. II 19–21.

Berenjian, A., Mahanama, R., Talbot, A., Regtop, H., Kavanagh, J., Dehghani, F., 2011b. Efficient media for high menaquinone-7 production: response surface methodology approach. New Biotechnol. 28, 665–672. https://doi.org/10.1016/j.nbt.2011.07.007.

Berenjian, A., Mahanama, R., Talbot, A., Regtop, H., Kavanagh, J., Dehghani, F., 2013. Effect of biofilm formation by *Bacillus subtilis natto* on menaquinone-7 biosynthesis. Mol. Biotechnol. 54, 371–378. https://doi.org/10.1007/s12033-012-9576-x.

Berenjian, A., Mahanama, R., Talbot, A., Regtop, H., Kavanagh, J., Dehghani, F., 2012. Advances in menaquinone-7 production by bacillus subtilis natto: fed-batch glycerol addition. Am. J. Biochem. Biotechnol. 8, 105–110. https://doi.org/10.3844/ajbbsp.2012.105.110.

Berenjian, A., Mahanama, R., Talbot, A., Regtop, H., Kavanagh, J., Dehghani, F., 2014. Designing of an intensification process for biosynthesis and recovery of menaquinone-7. Appl. Biochem. Biotechnol. 172, 1347–1357. https://doi.org/10.1007/s12010-013-0602-7.

Binkley, S.B., Maccorquodale, D.W., Thayer, A., Doisy, E.A., 1939. The isolation of vitamin K1. J. Biol. Chem. 130, 219–234.

Booth, S.L., 2012. Vitamin K: food composition and dietary intakes. Food Nutr. Res. 56 (1), 5505. https://doi.org/10.3402/fnr.v56i0.5505.

Cheng, K.C., Demirci, A., Catchmark, J.M., Puri, V.M., 2010. Modeling of pullulan fermentation by using a color variant strain of *Aureobasidium pullulans*. J. Food Eng. 98, 353–359. https://doi.org/10.1016/j.jfoodeng.2010.01.011.

Coban, B.C., Demirci, A., 2016. Enhancement and modeling of microparticle-added *Rhizopus oryzae* lactic acid production. Bioprocess Biosyst. Eng. 39, 323–330. https://doi.org/10.1007/s00449-015-1518-0.

Dam, H., 1935. The antihaemorrhagic vitamin of the chick: occurrence and chemical. Nat. Nat. 135, 652–653.

Ercan, D., Demirci, A., 2013. Current and future trends for biofilm reactors for fermentation processes. Crit. Rev. Biotechnol. 8551, 1–14. https://doi.org/10.3109/07388551.2013.793170.

Gast, G.C.M., de Roos, N.M., Sluijs, I., Bots, M.L., Beulens, J.W.J., Geleijnse, J.M., Witteman, C.J., Grobbee, D.E., Peeters, P.H.M., van der Schouw, Y.T., 2009. A high menaquinone intake reduces the incidence of coronary heart disease. Nutr. Metab. Cardiovasc. Dis. 19 (7), 504–510. https://doi.org/10.1016/j.numecd.2008.10.004.

Geleijnse, J.M., Vermeer, C., Grobbee, D.E., Schurgers, L.J., Knapen, M.H.J., van der Meer, I.M., Hofman, A., Witteman, J.C.M., 2004. Dietary intake of menaquinone is associated with a reduced risk of coronary heart disease: the Rotterdam study. J. Nutr. 134 (11), 3100–3105.

Goodman, S.R., Marrs, B.L., Narconis, R.J., Olson, R.E., 1976. Isolation and description of a menaquinone mutant from *Bacillus licheniformis*. J. Bacteriol. 125, 282–289.

Ho, K.G., Pometto, A.L.I., Hinz, P.N., Dickson, S., Demirci, A., 1997. Ingredient selection for plastic composite supports for L-(1)-lactic acid biofilm fermentation by *Lactobacillus casei* subsp. *rhamnosus*. Appl. Environ. Microbiol. 63, 2516–2523.

Howard, L.M., Payne, A.G., 2006. Health Benefits of Vitamin K2: A Revolutionary Natural Treatment for Heart Disease And Bone Loss, 1st ed. Basic Health Publications, Inc., Laguna Beach.

Ikeda, H., Doi, Y., 1990. A vitamin-K2-binding factor secreted from *Bacillus subtilis*. Eur. J. Biochem. 192, 219–224. https://doi.org/10.1111/j.1432-1033.1990.tb19218.x.

Kargi, F., 2009. Re-interpretation of the logistic equation for batch microbial growth in relation to Monod kinetics. Lett. Appl. Microbiol. 48, 398–401. https://doi.org/10.1111/j.1472-765X.2008.02537x.

Leh, M.B., Charles, M., 1989. Lactic acid production by batch fermentation of whey permeate: a mathematical model. J. Ind. Microbiol. 4, 65–70. https://doi.org/10.1007/BF01569695.

Luedeking, R., Piret, E.L., 1959. A kinetic study of the lactic acid fermentation. Batch process at controlled pH. Biotechnol. Bioeng. 1, 393–412. https://doi.org/10.1002/jbmte.390010406.

Mahanama, R., Berenjian, A., Regtop, H., Talbot, A., Dehghani, F., Kavanagh, J.M., 2012. Modeling menaquinone 7 production in tray type solid state fermenter. ANZIAM J. 53, 354–372.

Mahdinia, E., Demirci, A., Berenjian, A., 2017a. Production and application of menaquinone-7 (vitamin K2): a new perspective. World J. Microbiol. Biotechnol. 33, 2. https://doi.org/10.1007/s11274-016-2169-2.

Mahdinia, E., Demirci, A., Berenjian, A., 2017b. Strain and plastic composite support (PCS) selection for vitamin K (Menaquinone-7) production in biofilm reactors. Bioprocess Biosyst. Eng. 40, 1507–1517. https://doi.org/10.1007/s00449-017-1807-x.

Mahdinia, E., Demirci, A., Berenjian, A., 2018a. Optimization of *Bacillus subtilis natto* growth parameters in glycerol-based medium for vitamin K (Menaquinone-7) production in biofilm reactors. Bioprocess Biosyst. Eng. 41, 195–204. https://doi.org/10.1007/s00449-017-1857-0.

Mahdinia, E., Demirci, A., Berenjian, A., 2018b. Utilization of glucose-based medium and optimization of *Bacillus subtilis natto* growth parameters for vitamin K ( menaquinone-7) production in biofilm reactors. Biocatal. Agric. Biotechnol. 13, 219–224. https://doi.org/10.1016/j.bcab.2017.12.009.

Mahdinia, E., Demirci, A., Berenjian, A., 2018c. Enhanced Vitamin K (Menaquinone-7) production by *Bacillus subtilis natto* in biofilm reactors by optimization of glucose-based medium. J. Curr. Pharm. Biotechnol (In press).

Mahdinia, E., Demirci, A., Berenjian, A., 2018d. Effects of medium components in glycerol-based medium on vitamin K (menaquinone-7) production by *Bacillus subtilis natto* in biofilm reactors. Bioprocess Biosyst. Eng. https://doi.org/10.1007/s00449-018-2027-8. (In press).

Mahdinia, E., Demirci, A., Berenjian, A., 2018e. Implementation of fed-batch strategies for vitamin K (menaquinone-7) production by *Bacillus subtilis natto* in biofilm reactors. Appl. Microbiol. Biotechnol. 102 (21), 9147–9157. https://doi.org/10.1007/s00253-018-9340-7.

Mohammad, F.H.A., Badr-Eldin, S.M., El-Tayeb, O.M., El-Rahman, O.A., 1995. Polysaccharide production by *Aureobasidium pullulans* III. The influence of initial sucrose concentration on batch kinetics. Biomass Bioenergy 8, 121–129.

Pandey, A., 2003. Solid-state fermentation. Biochem. Eng. J. 13, 81–84. https://doi.org/10.1016/S1369-703X(02)00121-3.

Rahimi, M., Angelo, A.D., Gorski, C.A., Scialdone, O., Logan, B.E., 2017a. Electrical power production from low-grade waste heat using a thermally regenerative ethylenediamine battery. J. Power Sources 351, 45–50. https://doi.org/10.1016/j.jpowsour.2017.03.074.

Rahimi, M., Schoener, Z., Zhu, X., Zhang, F., Gorski, C.A., Logan, B.E., 2017b. Removal of copper from water using a thermally regenerative electrodeposition battery. J. Hazard Mater. 322, 551–556. https://doi.org/10.1016/j.jhazmat.2016.10.022.

Schurgers, L.J., Teunissen, K.J.F., Hamulyák, K., Knapen, M.H., Vik, H., Vermeer, C., 2007. Vitamin K-containing dietary supplements: comparison of synthetic vitamin K1 and natto-derived menaquinone-7. Blood 109, 3279–3283. https://doi.org/10.1182/blood-2006-08-040709.

Shahami, M., Ransom, R., Shantz, D.F., 2017. Synthesis and characterization of tin, tin / aluminum, and tin / boron containing MFI zeolites containing MFI zeolites. Microporous Misoporous Mater. 251, 165–172. https://doi.org/10.1016/j.micromeso.2017.05.049.

Singh, R., Puri, A., Panda, B.P., 2015. Development of menaquinone-7 enriched nutraceutical: inside into medium engineering and process modeling. J. Food Sci. Technol. 52, 5212–5219. https://doi.org/10.1007/s13197-014-1600-7.

Widhalm, J.R., Ducluzeau, A.L., Buller, N.E., Elowsky, C.G., Olsen, L.J., Basset, G.J., 2012. Phylloquinone (vitamin K1) biosynthesis in plants: two peroxisomal thioesterases of *Lactobacillales* origin hydrolyze 1,4-dihydroxy-2-naphthoyl-CoA. Plant J. 71, 205–215. https://doi.org/10.1111/j.1365-313X.2012.04972x.

Wu, W.J., Ahn, B.Y., 2011. Improved menaquinone (Vitamin K2) production in Cheonggukjang by optimization of the fermentation conditions. Food Sci. Biotechnol. 20, 1585–1591. https://doi.org/10.1007/s10068-011-0219-y.

Yamaguchi, M., 2006. Regulatory mechanism of food factors in bone metabolism and prevention of osteoporosis. Yakugaku Zasshi 126, 1117–1137. https://doi.org/10.1248/yakushi.126.1117.

Zwietering, M.H., Jongenburger, I., Rombouts, F.M., Van, T., Riet, K., 1990. Modeling of the bacterial growth curve. Appl. Environ. Microbiol. 56, 1875–1881 (doi: 0099-2240/90/061875-07$02.00/0).